Liquid Crystals
Publication details, including instructions for authors and subscription information:
http://www.informaworld.com/smpp/title~content=t713926090

Cholesteric liquid crystals as weathering indicators for marble surfaces

M. Koui[a]; A. Moropoulou[a]; K. Bisbikou[a]
[a] Chemical Engineering Department, Materials Science and Engineering Section, National Technical University of Athens, Zografou Campus, 9 Iroon Polytechniou Str., Zografou 15773, Athens, Greece,

Online publication date: 06 August 2010

To cite this Article Koui, M. , Moropoulou, A. and Bisbikou, K.(2000) 'Cholesteric liquid crystals as weathering indicators for marble surfaces', Liquid Crystals, 27: 12, 1561 — 1571
To link to this Article: DOI: 10.1080/026782900750037130
URL: http://dx.doi.org/10.1080/026782900750037130

LIQUID CRYSTALS, 2000, VOL. 27, NO. 12, 1561–1571

Cholesteric liquid crystals as weathering indicators for marble surfaces

M. KOUI*, A. MOROPOULOU and K. BISBIKOU

Chemical Engineering Department, Materials Science and Engineering Section,
National Technical University of Athens, Zografou Campus,
9 Iroon Polytechniou Str., Zografou 15773, Athens, Greece

(*Received 30 October 1998; in final form 27 September 1999; accepted 9 March 1999*)

Cholesteric liquid crystals have been used to study the weathered surfaces of marble from the Sanctuary of Demeter in Eleusis, near Athens. Previous investigations have shown that when a cholesteric phase is spread across the surface of the stone, the pitch of the mesophase is sensitive to the topography of the surface. The wavelength of the maximum in the reflected spectrum varies therefore with the microtexture of the surface. Small samples of surface stone from the temple which had been weathered in distinctive ways, were investigated in the laboratory. There appears to be a significant correlation between the optical reflectance spectra and the surface microtopography investigated by SEM, as indicated by computer aided analysis (Digital Image Processing). The results point to the development of an effective *in situ* method of monitoring the weathering of marble surfaces using cholesteric liquid crystals.

1. Introduction

Increasing interest in the protection of the cultural heritage has led to the need for accurate non-destructive techniques for the *in situ* investigation of the weathering of historic stone surfaces. It is especially important to be able to monitor the deterioration resulting from the polluted atmospheres of urban and industrial centres. We are particularly concerned with the weathering of the vulnerable white Pentelic marble (which was extensively used in classical Greek architecture) in heavily polluted atmospheres. A variety of weathering patterns has been studied [1]. The fine structure of the resulting crusts and encrustations depends on a combination of *intrinsic* factors, such as composition and microstructure, and *extrinsic* factors, such as the microenvironment and the chemical nature of the pollutants.

In previous investigations [2] it has been found that cholesteric phases applied directly onto the stone offer a sensitive and non-destructive way of characterizing the surface microstructure. The observed colour (i.e. the position of the maximum of the reflection band) is a sensitive indicator of surface microtexture [3–12], as expected by the general sensitivity of cholesteric phases to temperature [3–5], pressure [6–9], electric and magnetic fields [3–5, 10, 11] and to trace quantities of impurities [12]. In this case however, we suggest that it is the local curvature of the substrate surface within small pores which distorts the pitch in a characteristic fashion. The sensitivity of the colour change is extremely high in the neighbourhood of the cholesteric to smectic phase transition [4–10].

In our previous investigations it was shown that it is possible to characterize a variety of metal oxides with different microstructures [13–16], to distinguish marble surfaces from gypsum, and to identify where weathered gypsum (hydrated calcium sulphate) has undergone a transformation to calcium carbonate [2].

The most sensitive parameter for the shift of the wavelength, is $\Delta\lambda$, the difference $\lambda - \lambda'$, where λ and λ' are the wavelength at the peak of the diffuse reflectance spectrum, at the same temperature, for the mixture of cholesteric liquid crystals on the surface of the sorptive support and on the surface of blackened glass (sorptive inactive), respectively [14–17].

Regarding metal and metal oxide surfaces, formed under controlled conditions, the following empirical equation has been found to describe the variation of $\Delta\lambda$ with temperature, T, in °C and the sorptive properties:

$$(\lambda - \lambda')_T = (30.28 - 0.1T)S + [-121.3 \times 10^6/T^2 + 1351]$$

where the parameter S is a measure of the physical sorption of the substrate expressed in mg m^{-2} Methylene Blue [14–17].

In crusts and cementitious encrustations formed randomly on stone surfaces (under uncontrolled conditions) the above equation is not applicable because of difficulties in determining S by the Methylene Blue technique.

*Author for correspondence;
e-mail: markoue@orfeas.chemeng.ntua.gr

Liquid Crystals ISSN 0267-8292 print/ISSN 1366-5855 online © 2000 Taylor & Francis Ltd
http://www.tandf.co.uk/journals

The present work, which is part of an extensive research programme, aims to develop a liquid crystal weathering indicator for stone surfaces. In this context four different weathered and nearly cut Pendelic marbles surfaces [18, 19] (bare Pentelic marble, samples with washed out surfaces, with loose deposition on the surface and with cementitious encrustation) were studied by means of SEM and image analysis. Then the ability of liquid crystals to discriminate between these was investigated by measuring $\Delta\lambda$ vs. temperature and assessing its relation to the sorptive properties of the substrate.

The results obtained reveal a significant correlation between the visible diffuse reflectance spectra from the cholesteric mixture and the surface microtopography.

2. Experimental

2.1. *Weathered samples as substrates*

Sampling was performed in the Sanctuary of Demeter [18] at the archaeological site of Eleusis, situated in a highly aggressive industrial, urban and marine atmospheric environment in the vicinity of Athens, which causes the growth of characteristic crusts.

In our previous work [19], concerned with the investigation of weathering mechanisms in relation to particular characteristics of the materials/environment interface, a detailed classification of various types of crusts is given. Among them, the following more representative types of crust are used for the present study as well as bare Pentelic marble, see figure 1.

(1) Washed out surfaces.
(2) Black crust formations in the form of loose depositions.
(3) Cementitious encrustations on the horizontal marble surfaces.

For the spectrophotometric study, six samples were gathered for each type of crust and were cut into blocks $2 \times 1 \times 0.3\,\text{cm}^3$. The specimens were smoothed on the reverse face to give good contact with the thermostatic holder of the spectrophotometer. Samples of half this size were used for the SEM study.

2.2. *Pore structure and investigation methods*

The characterization of the pore structure includes the determination of the following parameters: (*a*) total porosity, (*b*) average pore radii, (*c*) pore size distribution (i.e. pore volume per average pore radius), (*d*) specific surface area as defined below [20, 21].

Among current techniques in use for pore structure investigation, scanning electron microscopy (SEM) was used in this work due to its nondestructive impact on the fragile crusts.

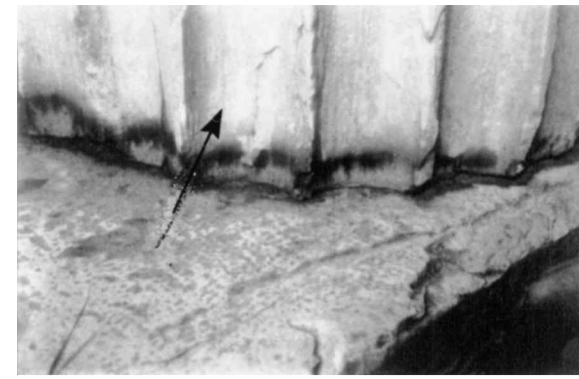

(*a*)

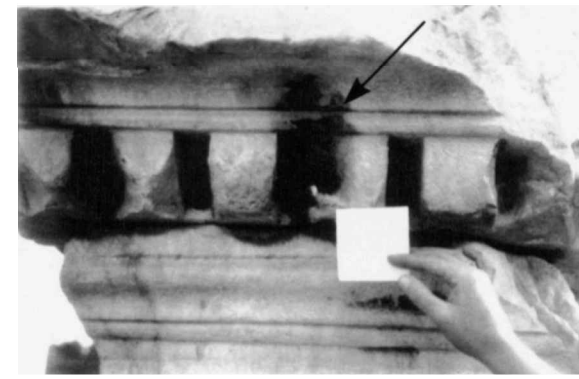

(*b*)

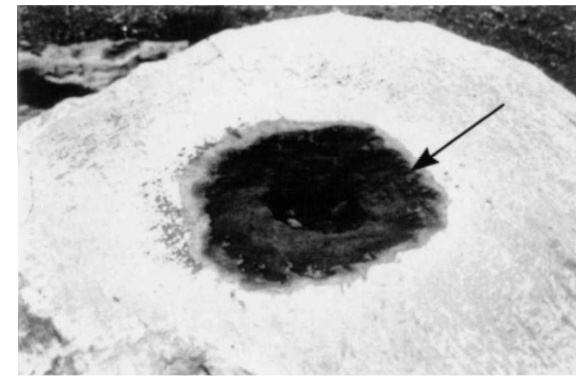

(*c*)

Figure 1. The various crust types under study: (*a*) washed out surfaces in direct contact with rainfall, (*b*) black crusts in the form of loose depositions on surfaces sheltered from rainwater, (*c*) cementitious encrustations pitting horizontal surfaces.

The SEM study was carried out with a Zeiss DSM 962 apparatus on specimens of size $1 \times 1\,\text{cm}^2$ for the fractured surfaces, with a magnification $\times 3000$. The SEM micrographs obtained ($16 \times 11\,\text{cm}^2$) allow a quantitative and statistical evaluation of the pore spaces [22] by image analysis [21].

The procedure used for the computer aided analysis by digital image processing is outlined in the following flow-sheet.

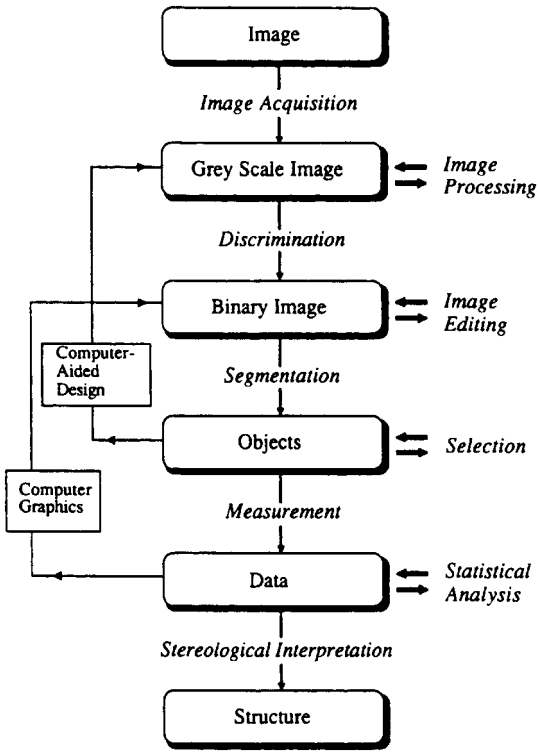

The SEM micrographs, after digitization, are processed by point operations, which alter the brightness of the pixels and increase the contrast between the pore space and the matrix (γ Factor). Then, by selecting the proper enhancement filter, random noise is removed from the image. By selecting the proper brightness threshold, the final image can be binarized into two regions, of different colours that distinguish the pores from the matrix.

The mean pore diameter (μm), the roundness of pore surfaces, the pore perimeter (μm), the pore surface area (μm^2), the fraction of the surface area covered by pores (%) and the total porosity defined below (%) are estimated by using the Image Pro Plus program [21].

The quantitative determination of porosity is obtained by relating the surface area to the volume using the Exner and Hougardy classical equation of quantitative stereometry [23]:

$V_V = L_L = A_A$, where $V_V = V/V_0$, V_0 is the reference volume of the sample and V is the volume of pores; $L_L = L/L_0$, where L_0 is the distance between two points on the reference surface and L is the sum of the particular lengths of the pores crossed by L_0; and $A_A = A/A_0$, where A is the surface area of the pores and A_0 is the reference surface area of the sample (figure 2).

Thus, total porosity is given by $A_A = A/A_0$, where A is the estimated surface area of the pores and A_0 the reference surface area of the sample as a total %.

The average pore diameters for a given surface area were estimated statistically by the approach of fitting the pores to circles of various diameters. This approach and the statistical evaluation is performed by using the image Pro Plus Program.

Pore size distribution, is shown by the histograms of the mean pore diameters versus the total pore surface area (%).

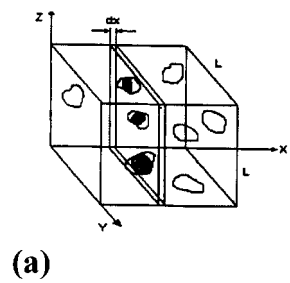

(a)

$$dV = Adx$$
$$V = \int_0^L dV = \int_0^L Adx$$
$$\overline{A} = 1/L \int_0^L Adx$$
$$V_V = V/V_0 = \overline{A}\,L/L^3$$
$$V_V = \overline{A}/A_0 = A_A$$

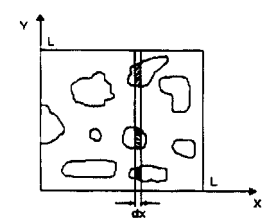

(b)

$$dA = Ldx$$
$$A = \int_0^L dA = \int_0^L Ldx$$
$$\overline{L} = 1/L \int_0^L Ldx$$
$$A_A = A/A_0 = \overline{L}\,L/L^2$$
$$A_A = \overline{L}/L_0 = L_L$$

Figure 2. Postulation of the basic quantitative stereometric equations by Exner and Hougardy (*a*) $V_V = A_A$, (*b*) $A_A = L_L$.

Since a circle is the shape with the minimum perimeter for a given surface area, roundness is directly related to the specific surface area of the pores. An estimate of the

Table 1. Wavelength and mean values (nm) of light selectively reflected by bare Pentelic marble surfaces at several temperatures.

	Temperature/°C			
	25	26	27	28
	586	488	450	430
	614	499	446	423
	580	479	434	420
	635	490	436	418
	604	484	438	427
	572	496	441	415
Mean	599	489	441	422
SD	± 22	± 7	± 6	± 5

Table 2. Wavelength and mean values (nm) of light selectively reflected by washed out surfaces at several temperatures.

	Temperature/°C			
	25	26	27	28
	635	494	446	430
	611	488	443	424
	604	505	448	425
	617	496	444	423
	645	510	453	427
	667	497	458	434
Mean	630	498	449	427
SD	± 24	± 8	± 6	± 4

Table 3. Wavelength and mean values (nm) of light selectively reflected by loose deposition formations at several temperatures.

	Temperature/°C			
	25	26	27	28
	679	523	462	434
	750	557	480	440
	700	531	472	434
	665	528	461	432
	618	517	470	430
	665	524	463	432
Mean	680	530	468	434
SD	± 44	± 14	± 7	± 3

Table 4. Wavelength and mean values (nm) of light selectively reflected by cementitious surface encrustations at several temperatures.

	Temperature/°C			
	25	26	27	28
	730	570	480	452
	676	510	460	428
	750	580	500	464
	718	545	473	430
	674	507	454	423
	725	559	485	440
Mean	712	545	477	440
SD	± 31	± 31	± 17	± 16

Table 5. Mean wavelength values (nm) of selectively reflected light at several temperatures for the various substrates, and the values of $\Delta\lambda = \lambda - \lambda'$.

	Temperature/°C			
Specimen type	25	26	27	28
λ (nm) mean values of 6 measurements				
Bare Pentelic marble	599	489	441	422
Washed out surfaces	630	498	449	427
Loose depositions	680	530	468	434
Cementitious encrustation	712	545	477	440
Blackened Glass (λ′)	515	451	423	411
λ-λ′ (nm)				
Bare Pentelic marble	84	38	18	11
Washed out surfaces	115	47	26	16
Loose depositions	165	79	45	23
Cementitious encrustation	197	94	54	29

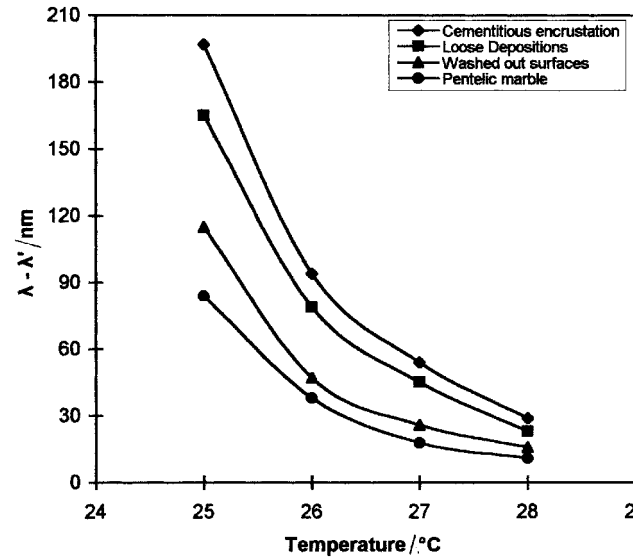

Figure 3. $(\lambda - \lambda')$ vs. temperature for each substrate type.

pore 'roundness', according to quantitative stereometry, is expressed as the ratio:

$$(\text{perimeter})^2/4\pi \times (\text{surface area})a$$

which expresses the deviation of pore shape from a circle. Roundness distribution is shown by a histogram of the roundness of the pore surface area versus the pore percentage.

For a perfect circle the value of the roundness parameter is 1. As the value of roundness increases, a larger specific surface area for a given pore is indicated.

2.3. *Liquid crystals materials, application procedure and wavelength measurement*

On the surface face of all the samples (bare marble and weathered specimens) a solution of cholesteric

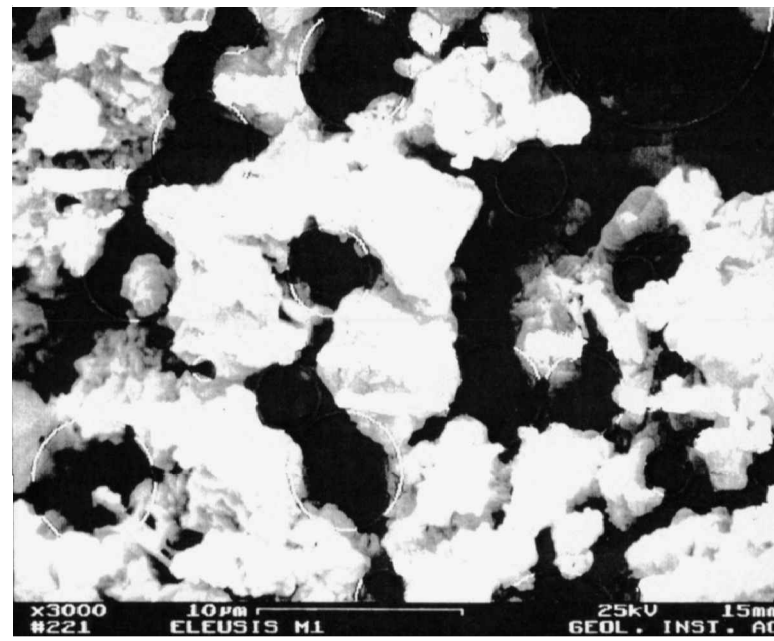

(*a*)

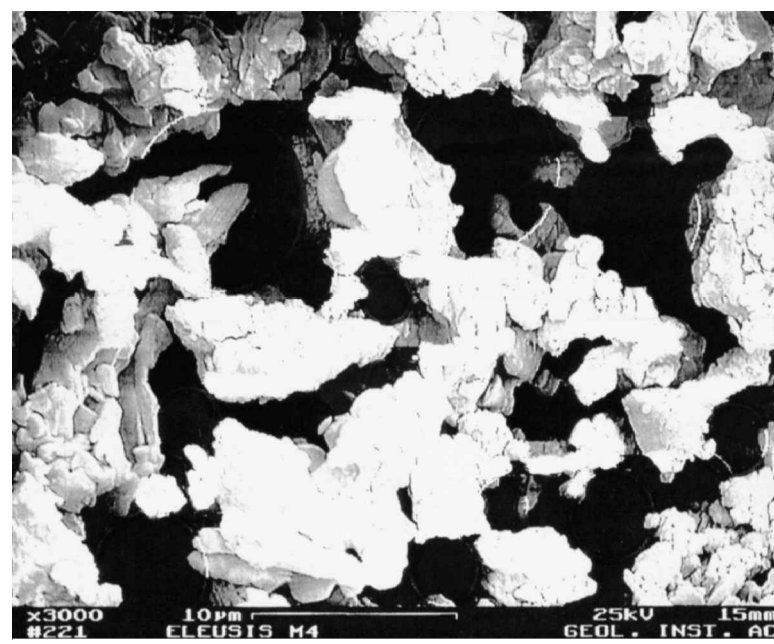

(*b*)

Figure 4. Scanning electron microscopy observations of: (*a*) washed out surfaces, (*b*) loose depositions, (*c*) cementitious encrustations, all × 3000.

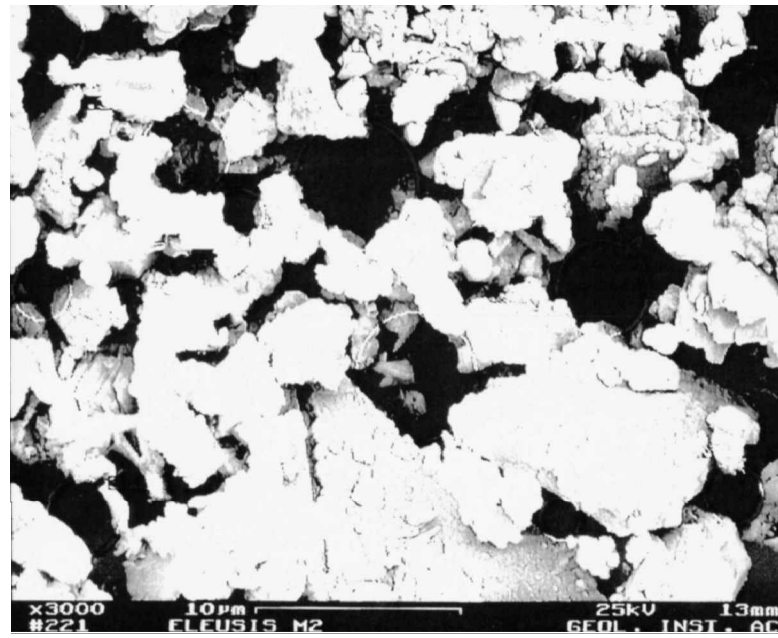

Figure 4. (*continued*). (*c*)

mixture (1:4 ratio by wt of cholesteryl 4-carbomethoxyoxybenzoate and cholesteryl oleyl carbonate, 10% w/v in diethyl ether) was spread in such a way as to ensure a uniform thickness (50–60 µm) of the mixture after evaporation of the solvent.

The complete evaporation of the diethyl ether was assumed by heating the samples (placed horizontally on a thermostatic plate) above the isotropic transition point (35°C). Then the sample was allowed to cool and was manipulated (e.g. sheared) mechanically to give the Grandjean microstructure.

Visible diffuse reflectance spectra [2, 14–17] at several temperatures (25, 26, 27 and 28°C) were obtained from all the types of specimens, covered with the above mentioned cholesteric mixture, as well as from the inactive surface of blackened glass used as reference. The measurements were carried out with a Perkin-Elmer double beam spectrophotometer (model Lamda 3 UV/VIS) for visible light, with an integrating sphere attachment (Perkin-Elmer Type R453). Each specimen, with the cholesteric mixture, was placed on a special thermostatic block-heater and introduced into the apparatus (in the compartment designed for back reflection measurements) lying normal to the light beam. Visible diffuse reflectance spectra were taken at each predetermined temperature. The accuracy of the wavelength measurements was ± 0.5 nm and the temperature was accurate to ± 0.1°C. Measurements were taken for six specimens of each type of crust and at each temperature; the mean value of λ was calculated in nm. From these mean values, the peak (λ') obtained from the liquid crystal mixture on a blackened glass plate for each different temperature was subtracted [2, 14, 15, 17].

3. Results and discussion

The results derived from the spectral measurements (tables 1–4) reveal different values of $\Delta\lambda$ for the different types of crusts and the bare marble specimens. The selective reflected wavelength peaks for the six measurements on each type of crust in the temperature range 25–28°C, as well as the mean values and the standard deviations are also shown in these tables.

In table 5, the mean wavelength values (nm) per substrate at the various temperatures are given, reduced by the mean values (λ') for the reference substrate (blackened glass) in the same temperature range. The values are reported to enable comparison between the behaviour of bare and weathered surfaces. Figure 3 presents plots obtained from the values of table 5.

The selectively reflected light band values at the same temperature, for the four types of specimen studied increase in the following series:

Bare marble surfaces < Washed out surfaces < Loose deposition formations < Cementitious encrustations.

The shift of the selectively reflected light band to longer wavelength as the cholesteric structure progressively unwinds is expected to follow the increased sorptive abilities of the solid supports (crusts).

Physical sorption on the various substrates relates to the contact surface of the solid/liquid interface [24] depending on: the direct total crust surface area (estimated as $A_c\% = (A_o - A)/A_o$); the total pore surface area $A_A\%$; and the specific surface area of the pores, inversely proportional to the pore radii and directly proportional to the roundness.

The textural and microstructural characteristics of the crusts investigated by SEM and elaborated by DIP [25] are presented in figures 4(*a–c*) and 5(*a–c*), respectively. The microstructural characteristics determining the sorptive abilities of the substrates are estimated for the various crusts and are shown in table 6.

The total crust surface A_c (%) is estimated by subtracting the total pore surface A_A (%) from the total reference surface A_o under study.

The average pore diameter is estimated by the histograms of pore size distribution per crust, figures 6(*a*),

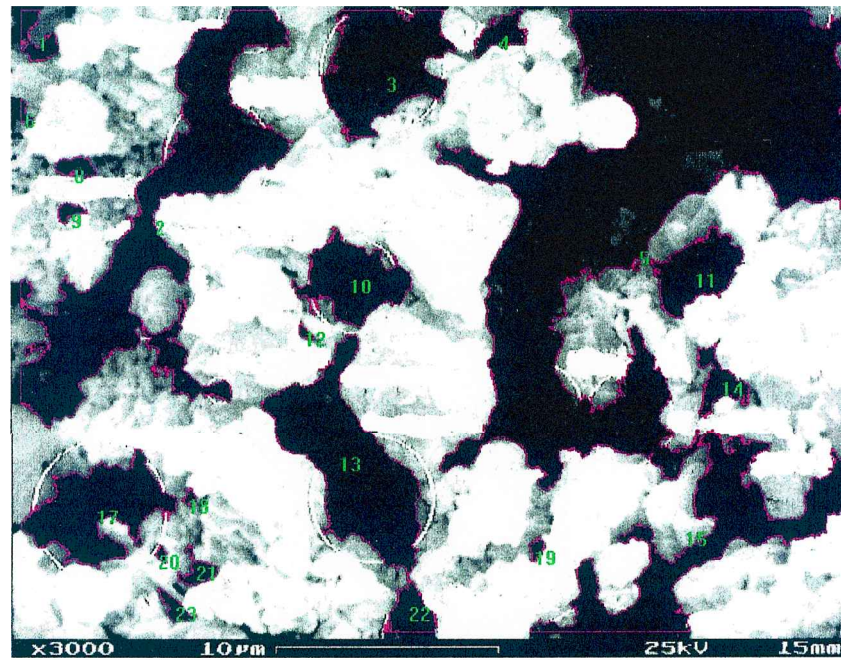

(*a*)

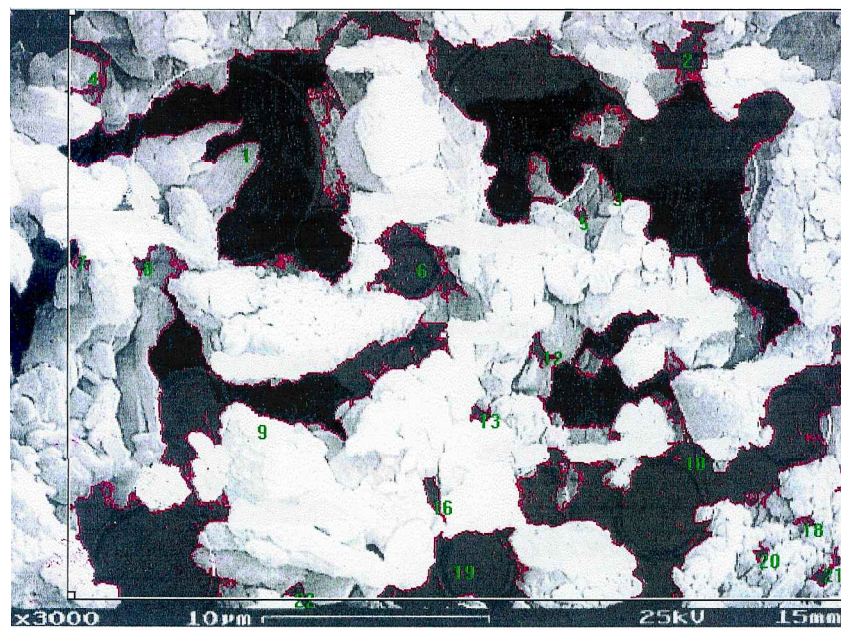

(*b*)

Figure 5. Digital image processing to estimate microstructural characteristic of: (*a*) washed out surfaces, (*b*) loose depositions, (*c*) cementitious encrustations.

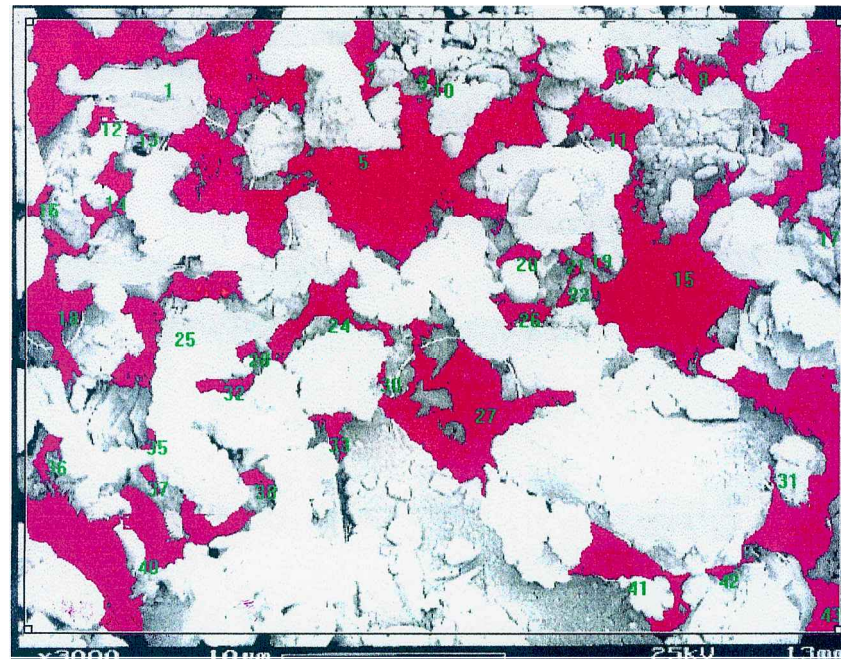

(*c*)

Figure 5. (*continued*).

Table 6. Estimated microstructural characteristics of various crusts.

Crust type	Total pore surface A_A/%	Total crust surface A_C/%	Average pore Diameter/μm
Washed out	35.46	64.54	7.6
Loose depositions	32.54	67.56	3.8
Cementitious encrustations	25.55	74.45	2.2

7 (*a*), 8 (*a*). The roundness distribution per crust is shown in figures 6 (*b*), 7 (*b*), 8 (*b*).

In table 6 and figures 6–8 one may observe the following textural and microstructural characteristics regarding the crusts under study.

3.1. *Washed out surface*

This has the highest total pore surface area A_A = 35.46% and the highest average pore diameter 7.6 μm. The pore size distribution deviates from normal and shows that more than 70% of the total pore surface is attributed to large pores between 10 and 12 μm, while intermediate pore diameters are absent. The existence of mainly large pores, together with low average roundness (ranging between 1 to 6 for 15% of the pores) indicates a relatively small specific surface area and implies the relatively small physical sorptive ability of the smallest total crust surface A_c, estimated at 64.54%.

3.2. *Loose deposition formations*

These have an intermediate total pore surface A_A = 32.54% and average pore diameter (3.8 μm). The pore size distribution presents a gradation from small to large pores, while 45% of the total pore surface is attributed to large pores > 14 μm. However, the higher roundness values (ranging between 2 and 6 for 40% of the pores and between 8 and 20 for 30% of the pores) along with the asymmetric distribution, account for the relatively

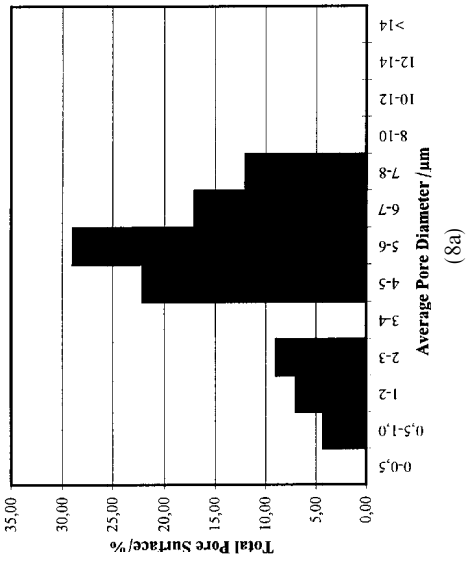

(8a)

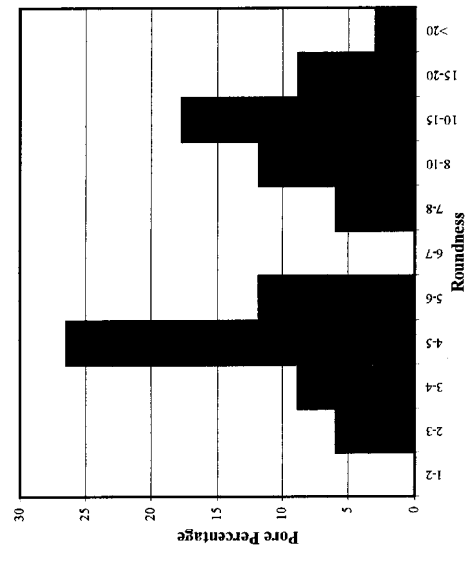

(8b)

Figure 8. (*a*) Histogram of pore size distribution for cementitious encrustations. (*b*) Histogram of pore roundness distribution for cementitious encrustations.

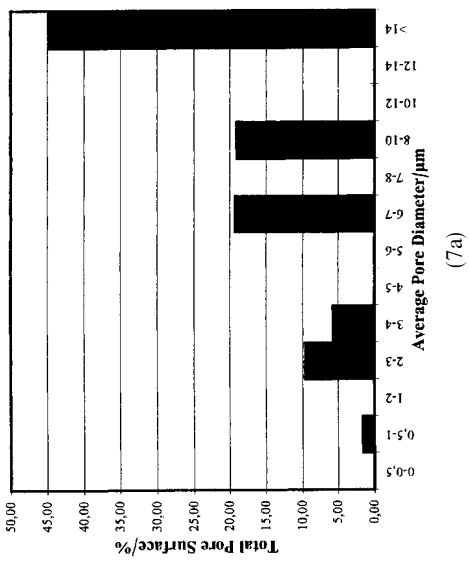

(7a)

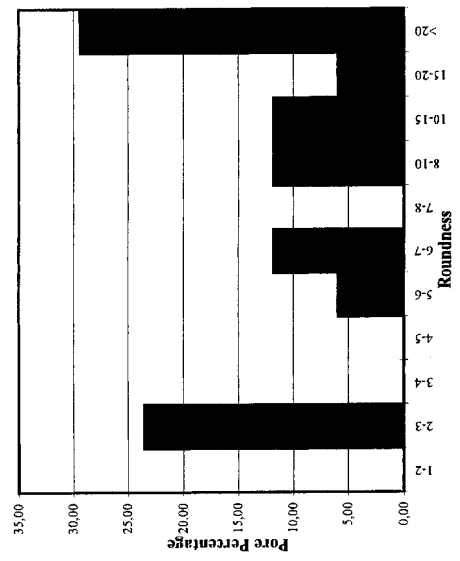

(7b)

Figure 7. (*a*) Histogram of pore size distribution for loose depositions. (*b*) Histogram of pore roundness distribution for loose depositions.

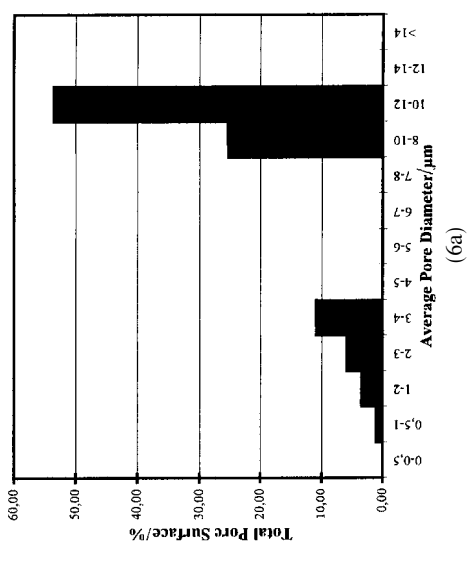

(6a)

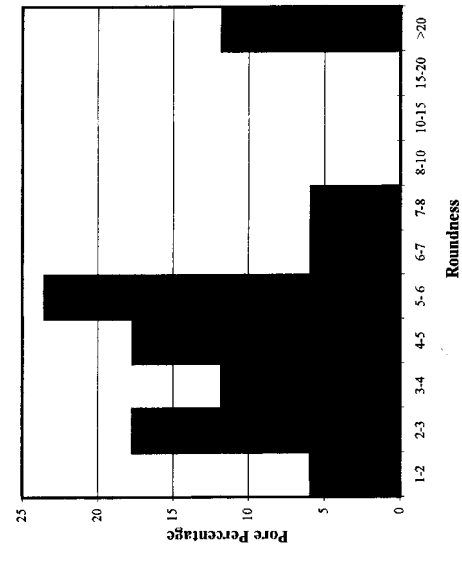

(6b)

Figure 6. (*a*) Histogram of pore size distribution for washed out surfaces. (*b*) Histogram of pore roundness distribution for washed out surfaces.

higher specific surface area, which implies a relatively higher physical sorptive ability of the total crust surface A_c, estimated at 67.46%.

3.3. *Cementitious encrustations*

These have the lowest total pore surface $A_A = 25.55\%$ and average pore diameter (2.2 μm). The pore size distribution is normal, with 50% of the total pore surface attributed to small pores (4–6 μm). This, along with the relatively high average of roundness values of 11.47, with large deviations, implies the relatively higher physical sorptive ability of the larger total crust surface A_c, estimated at 74.45%.

According to these results, the differentiation of the selectively reflected wavelength values can be attributed to the different textures and microstructures of the three types of crust. This is in agreement with their different chemical compositions and mechanisms of growth [19] as also illustrated in figures 9(*a–c*) by the SEM investigation of cross sections in depth.

In particular, the sorptive properties of the crusts increase, while the specific surface area increases. This leads to different shifts of the selectively reflected light band from the cholesteric mixture in the same sequence:

Washed out surfaces < Loose deposition formations < Cementitious encrustations.

4. Conclusions

From the results derived from the present research we conclude that a technique involving the measurement of the position of the maximum in the reflection spectrum of an applied layer of cholesterol liquid crystals can be developed to produce a viable, quantitative indication of the weathering patterns of marble surfaces.

Acknowledgements are attributed to Prof. B. Fitzner (Geological Institute of Aachen Technical University) for the SEM observations of the crusts and to Chem. Eng. V. Tsantila for the Digital Image Processing to assess their porosity. This work is part of the EC Program in the field of the Environment, Contract No. EV5V-CT92-0102, 1993 (Scientific Coordinator Prof. F. Zezza, Istituto di Geologia Applicata e Geotecnica, Facolta di Ingegneria, Politecnico di Bari, Italy.

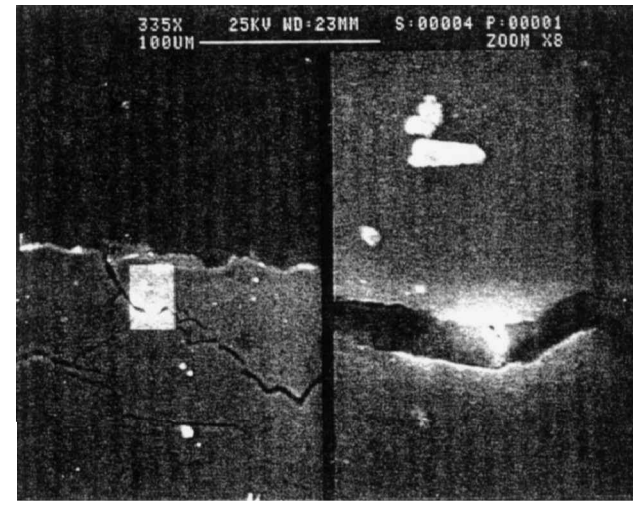

(*a*)

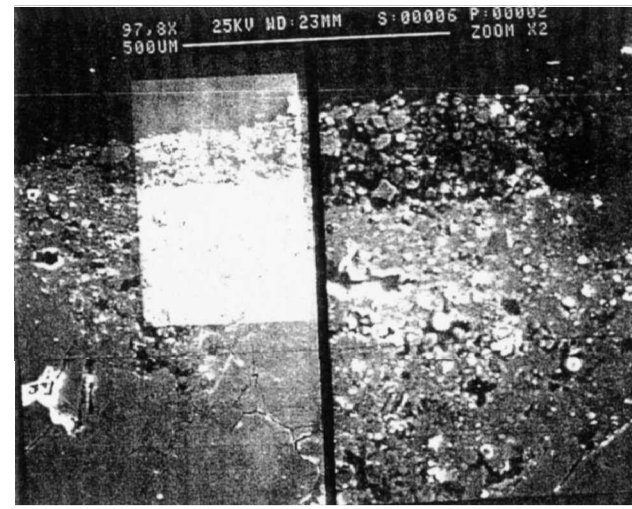

(*b*)

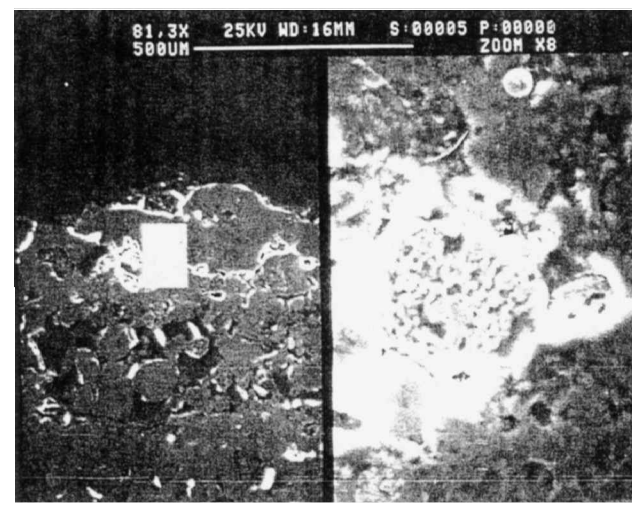

(*c*)

Figure 9. SEM observations of cross sections showing the microstructure of the crusts in depth. (*a*) Microfractured crusts of the washed out surfaces. (*b*) The two layers of gypsum crystal formation of the loose deposits; the outer one is the more porous. (*c*) The cementitious encrustation composed of hydraulic formations with a microstructure of small pores and high roundness.

References

[1] Moropoulou, A., Koui, M., Theoulakis, P., Kourteli, Ch., and Zezza, F., 1995, *J. environ Chem Technol*., **1,** 23.

[2] Skoulikidis, Th., Koui, M., and Kostoudi, 1991, *Mol. Cryst. liq. Cryst*., **206,** 117.

[3] De Gennes, P. G., 1974, *The Physics of Liquid Crystals* (Oxford: Clarendon Press).

[4] Brown, G. H., 1976, *Advances in Liquid Crystals*, Vol. 2 (New York: Academic Press).

[5] Brown, G. H., 1977, *J. Colloid interface Sci*., **58,** 534.

[6] Kayes, P. H., Weston, H. T., and Daniels, W. B., 1973, *Phys. Rev. Lett*., **31,** 628.

[7] Polmann, P., and Stegemeyer, H., 1974, *Ber. Bunsenges. Phys. Chem*., **78,** 843.

[8] Polmann, P., 1974, *Ber. Bunsenges. Phys. Chem*., **78,** 374.

[9] Polmann, P., 1974, *J. Phys. E*., **7,** 490.

[10] Meier, G., Sackmann, E., and Gradmaier, J. G., 1975, *Applications of Liquid Crystals* (Berlin: Springer-Verlag).

[11] Khoo, I.-C., and Wu, S.-T., 1993, *Optics and Nonlinear Optics of Liquid Crystals*, Vol. VI (Singapore: World Scientific).

[12] Gray, G. W., and Winsor, P. A., (editors), 1974, *Liquid Crystals and Plastic Crystals* (Chichester: Ellis Horwood).

[13] Skoulikidis, Th., and Koui, M., 1980, *Mol. Cryst. liq. Cryst*., **61,** 31.

[14] Skoulikidis, Th., and Koui, M., 1981, *Scuola sui Crystalli Liquidi*, UNICAL-81 proceedings, p. 569.

[15] Skoulikidis, Th., and Koui, M., 1983, *Mol. Cryst. liq. Cryst*., **95,** 323.

[16] Koui, M., Karayannis, H., and Kartsonakis, M., 1997, *Liq. Cryst*., **22,** 567.

[17] Skoulikidis, Th., Koui, M., and Skotaras, N., 1997, *Mol. Cryst. liq. Cryst*., **300,** 65.

[18] Moropoulou, A., Bisbikou, K., Cristaras, B., Kassoli Fournaraki, A., Zouros, N., Makedon, Th., Fitzner, B., and Heinrichs, K., 1995, *Bolettino Geofisico*, **18,** 37.

[19] Moropoulou, A., Bisbikou, K., Torfs, K., van Grieken, R., Zezza, F., and Macri, F., 1998, *Atmos. Environ*., **32,** 967.

[20] Moropoulou, A., and Bisbikou, K., 1998, *Environmental Technology*, (Selper Ltd.), p. 19.

[21] Simwonis, D., Naoumidis, A., Dias, F. J., Linke, J., and Moropoulou, A., 1997, *J. Mater. Res*., **12,** 1508.

[22] Fizner, B., and Basten, D., 1992, *Gesteinporositat-klassifizierung, messtechnische Erfassung und Bewertung ihrer Verwitterungsrelevanz*, Annual report on the research program on stone decay and stone conservation, 4: 19–32, (Ernst and Sohn Berlin).

[23] Exner, H. E., and Hougardy, H. P., 1986, *Einfuhrung in die Quantitative Gefugeanalyse Informationsgesellschaft* (Verlag).

[24] Atkins, P. W., 1989, *Physical Chemistry*, 3rd Ed (Oxford: Oxford University Press).

[25] Wolberg, G., 1992, *Digital Image Warping* (IEEE Computer Society Press).